Short Communication:

Structural Elucidation, Antioxidant Properties, and *In Silico* Molecular Docking of Schiff Base Complexes Derived from Naphthalene-1,8-diamine and Terephthalaldehyde

Chanar Ahmed Hussein, Khansaa Shakir Al-Nama*, and Ammar Abdulsattar Ibrahim

Department of Chemistry, College of Science, University of Mosul, Left Bank, Mosul, Nineveh 41001, Iraq

* ***Corresponding author:***

email:
khnsaash.al-nama@uomosul.edu.iq

Received: April 15, 2025
Accepted: June 30, 2025

DOI: 10.22146/ijc.106001

Abstract: *By combining two mmol of naphthalene-1,8-diamine with one mmol of terephthalaldehyde, a TPAL-DAN ligand was synthesized. Six metal salts: Mn(II), Co(II), Ni(II), Cu(II), Zn(II), and Cd(II) were used to prepare six Schiff base complexes. The structure of the Schiff base (TPAL-DAN) was confirmed by FTIR, ^{1}H- and ^{13}C-NMR spectroscopy, mass spectrometry, and elemental analysis. Its complexes were confirmed through CHN analysis, FTIR, UV-vis spectroscopy, magnetic moment, and molar conductivity measurements. The spectral results indicate that the ligand exhibits tetradentate behavior in all six complexes, which are dinuclear metal(II) complexes, and tetrahedral geometries are observed in each metal complex. FTIR data show a lower frequency of the azomethine group in complexes than in the ligand. X-ray powder diffraction of chelates (1–4) confirms several diffraction peaks indicating the crystal system in the prepared complexes. All complexes'* in vitro *antioxidant capacities were estimated using DPPH free radical scavenging assays. Docking studies were conducted to predict the efficacy of the newly synthesized compounds with a breast cancer-associated protein (ID: 4jlu) and an anti-inflammatory target (ID: 1oxr). The binding energies were varied from −6.1437 to −8.1601 kcal/mol and −6.8850 to −9.9667 kcal/mol, respectively. These results highlight the potential of TPAL-DAN complexes as bioactive agents.*

Keywords: *naphthalene diamine; Schiff base; DPPH;* in vitro; in silico

■ INTRODUCTION

In 1970, Robson used the term "dinucleating ligands" to refer to a class of polydentate chelating ligands that can bind to two metal ions simultaneously [1-2]. Because they offer increased stability and keep the two metal centers close together, these ligands are especially well-suited to produce binuclear metal complexes [3]. This spatial arrangement has significant implications for metal-metal interactions and the reactivity of the resulting complexes [3-4]. Transition metals such as Fe^{2+}, Fe^{3+}, Zn^{2+}, and Cu^{2+}, generally serving as components of proteins and enzymes or as activators of enzymes, are considered to be critical players in many vital biological processes, including oxygen transport, energy production, neurotransmission, regulation of gene expression, and synthesis of essential molecules [5-6]. This configuration is critical for achieving specific reactivity and selectivity in biochemical transformations. Adding particular donor elements, such as oxygen, nitrogen, or sulfur, to structural frameworks allows for simultaneous coordination with two metal centers.

Schiff bases can be modified to create binuclear transition metal complexes and are utilized in various fields like electrochemistry, bio-inorganic chemistry, separation processes, photodegradation, pharmacy, antimicrobial applications, and dyes due to their ability to form stable complexes with metal ions, properties due to the chelating effect [7]. These ligands often feature bridging groups or spatial arrangements that mimic the binuclear active sites found in proteins and enzymes, thereby promoting the proximity of the metal ions and enhancing their functionality in various biological and

catalytic applications [8]. Tetradentate Schiff bases, which possess four donor sites, are integral components in coordination chemistry due to their versatile binding ability and stability in the metal complexes. Their structural flexibility allows them to coordinate in various geometric configurations, making them ideal for applications in catalysis, material science, and biological systems [9-10]. The ability of this type of ligand to impart specific electronic and magnetic properties to the metal centers further enhances their importance in diverse medicinal applications such as antibacterial, antimalarial, antifungal, antitubercular, anticancer, and anti-inflammatory metal-based medicines [11-12]. Therefore, in the present work, the ligand was prepared from the condensation of two mmol of naphthalene-1,8-diamine with one mmol of terephthalaldehyde (TPAL-DAN). The Schiff base reacted with various metal (II) chlorides, such as Mn(II), Co(II), Ni(II), Cu(II), Zn(II), and Cd(II) to prepare metal complexes. All synthesized compounds were characterized by Fourier transform-infrared (FTIR), mass spectrometry (MS), ultraviolet-visible (UV-vis) spectroscopy, elemental analysis, and various physicochemical methods. All the newly synthesized compounds were screened for their antioxidant properties. Furthermore, simulations of molecular docking studies were conducted to predict the efficacy of the newly compounds with a breast cancer-associated protein (PDB ID: 4jlu) and an anti-inflammatory target (PDB ID: 1oxr).

■ EXPERIMENTAL SECTION

Materials

The Aldrich Chemical Company provided terephthalaldehyde and naphthalene-1,8-diamine, which were used directly without additional purification. Purchased from Sigma, the metal salts were utilized without further purification. The organic solvents, such as ethanol, dimethylformamide (DMF), and dimethyl sulfoxide (DMSO), were provided by BDH Company. Before use, all solvents underwent standard purification procedures.

Instrumentation

NMR spectra were captured using a Bruker Analytic 300 MHz spectrometer and DMSO-d_6 as the solvent. A BRUKER was used to acquire FTIR spectra covering the 400–4000 cm^{-1} range. A Thermo Fisher Eager 300 was used to do elemental analysis. Using quartz cells and DMSO as the solvent, UV-vis spectral measurements were performed using a Perkin Elmer Lambda 365 spectrophotometer. The Agilent 5975C was used to record the MS in positive ion mode. Biological assay, which is the 2,2-diphenyl-1-picrylhydrazyl (DPPH) assay, was used to determine the antioxidant activity of the synthesized compounds. Using PHILIPS, PW1730, XRD was measured on powdered samples. Studies utilizing atomic absorption spectroscopy (AAS) were conducted with a Shimadzu 760. The melting point was recorded using a DMP-800/DMP-600 device in a capillary tube. Electrical connection was measured in DMSO solvent, and magnetic susceptibility was measured via magnetic susceptibility balance (Mark 1MSB), Sherwood Scientific UK.

Procedure

Preparation of azomethine ligand (Schiff bases)

The Schiff base ligand (TPAL-DAN) was synthesized by reacting (0.316 g, 2 mmol) of 1,8-diaminonaphthalene with (0.134 g, 1 mmol) of terephthalaldehyde in 20 mL of absolute ethanol with 2–3 drops of 0.1 M hydrochloric acid as a catalyst. The mixture was heated under reflux and stirred at 70 °C for about 6 h. After cooling, the product was filtered, washed with cold water and ethanol (7:3 v/v), dried, and stored in an airtight desiccator [13-14]. The Schiff base ligand was confirmed by thin layer chromatography (TLC), R_f = 0.86 (EtOAc:Hex:DCM 2:7:1 v/v/v); the pathway is shown in Scheme 1.

Synthesis of binuclear complexes

The synthesis of binuclear Schiff base complexes involved combining 0.414 g (1 mmol) of TPAL-DAN with 0.395, 0.476, 0.475, 0.340, 0.272, and 0.402 g (2 mmol each) of $MnCl_2{\cdot}4H_2O$, $CoCl_2{\cdot}6H_2O$, $NiCl_2{\cdot}6H_2O$, $CuCl_2{\cdot}2H_2O$, $ZnCl_2$, $CdCl_2{\cdot}H_2O$ sequentially in 20 mL of absolute ethanol as the reaction medium [13-14]. The mixture was refluxed until a distinct colored precipitate formed. Upon cooling at room temperature, the solid product was isolated by filtration. After being repeatedly cleaned with cold ethanol, it was left to dry in a vacuum

desiccator at a lower pressure. The preparation pathway is shown in Scheme 1.

DPPH radical scavenging

An effective and widely used method for evaluating free radical neutralization is the DPPH radical scavenging assay. This was used to carefully assess the antioxidant activity of the produced compounds [15-16]. To reach the required concentration, the ligand and its matching coordination complexes with Co(II), Mn(II), Cu(II), Ni(II), Cd(II), and Zn(II) ions were dissolved in a small quantity of DMF and then diluted in ethanol. As strong donors of hydrogen atoms, these complexes efficiently squelch DPPH radicals and cause a noticeable colorimetric shift from deep violet to pale yellow. This occurrence shows that the DPPH radical has been reduced to a non-radical state.

The scavenging efficiency of the radicals was quantitatively measured at 517 nm using a UV-vis spectrophotometer. The percentage of radical scavenging ability was calculated using Eq. (1);

$$\text{DPPH scavenging}(\%) = \%\text{Inhibition} = \frac{A_0 - A_1}{A_0} \times 100\% \quad (1)$$

where A_0 was the absorbance of the control reaction and A_1 was the absorbance in the presence of a test or standard sample.

Molecular docking

Molecular docking provides a powerful tool for understanding the degree of recognition between the tested compounds and the amino acids of the enzyme's active site. These molecular docking highlight the candidates' bioactivities. The RCSB (https://www.rcsb.org) Protein Data Bank was used to obtain the 3D structures of the protein targets, as shown in Fig. 1. These files were sent to the Molecular Operating Environment (MOE) 2015 software, where they were modified to add polar hydrogen atoms and remove water molecules and other molecules [17-18]. The 3D structure of the ligand and its complexes and conformations were created using the ChemAxon Marvin Sketch 5.3.735 program, saved in mol2 format,

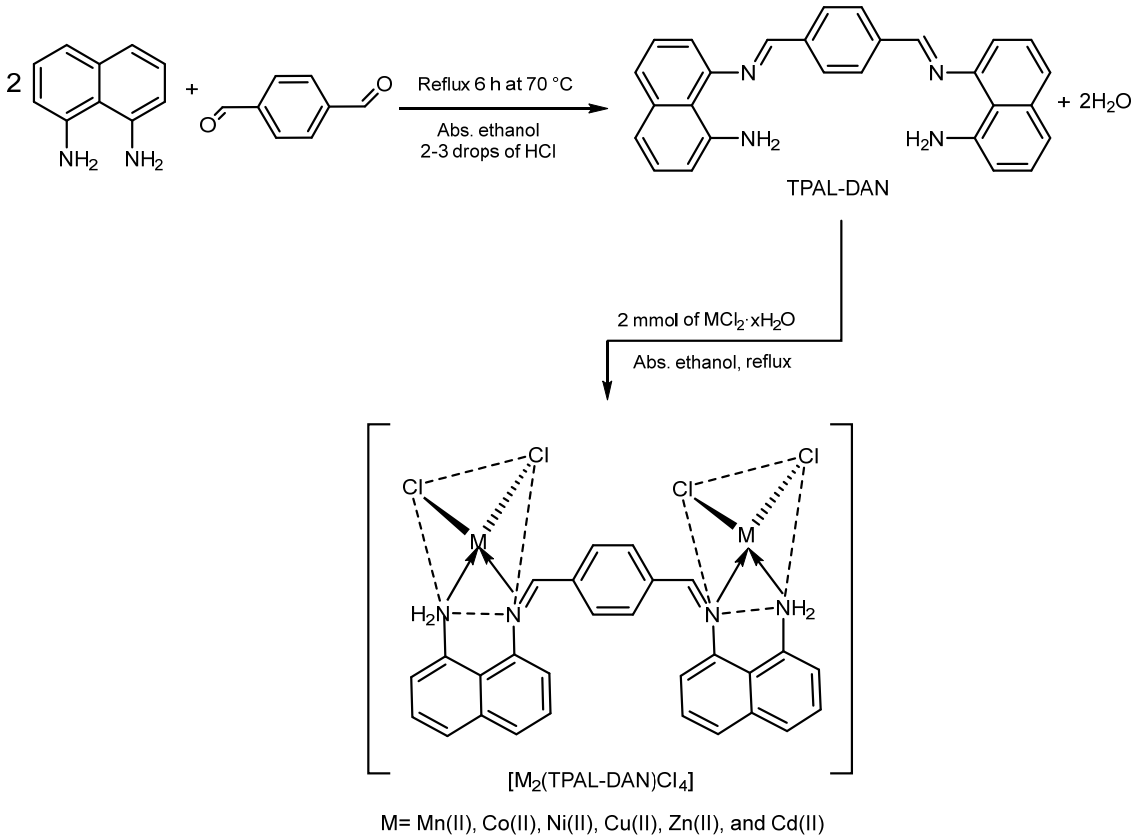

Scheme 1. Synthesis route of the ligand and its complexes

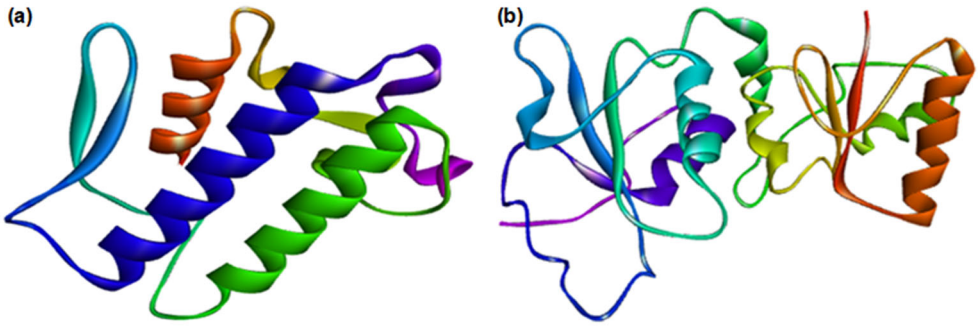

Fig 1. The visualization of 3D structure of (a) 1oxr and (b) 4jlu proteins

then converted to the MOE software. The molecular docking analysis was carried out using the MOE. To determine the binding energy between the ligand and its complexes (medicines) with a cancer-associated protein (4jlu), on the other hand, and with the receptor anti-inflammatory target (1oxr), the results were assessed. The MOE program was utilized to visualize the protein-ligand complexes [19-20]. After characterizing the polar and hydrophobic interactions between the ligand and the target, 2D representations of these interactions were created.

■ RESULTS AND DISCUSSION

Conductivity Measurements

The ligand was created by carefully optimizing the condensation reaction under controlled conditions between naphthalene-1,8-diamine and terephthalaldehyde to produce the Schiff base ligand, previously shown in Scheme 1. Its complexation with metal chlorides was successfully achieved, demonstrating a stoichiometric metal-to-ligand ratio of 2:1. Conductivity measurements in DMSO for complexes with low conductivity have values below 50 Ω^{-1} cm^2 mol^{-1}, while in complexes with high conductivity exceed 50 Ω^{-1} cm^2 mol^{-1}. This study's conductivity values ranged from 5.0 to 20.6 Ω^{-1} cm^2 mol^{-1}, as shown in Table 1. The physical properties of the compounds, including elemental analysis, coloration, and melting points, have been thoroughly described [21-22]. These properties have provided a deep understanding of their properties and molecular structures, as shown in Table 1.

Table 1. The CHN analysis, conductivity, and physical properties of the ligand and its complexes

Compounds	Color	M.p. (°C)	Yield %	Molecular weight (g/mol)	Elemental analysis (%) Found (calc)				ΛM (Ω^{-1} cm^2 mol^{-1})
					C	H	N	M	
$C_{28}H_{22}N_4$(TPAL-DAN)	White	185–187	80	414.51	81.13 (80.98)	5.35 (4.84)	13.52 (12.08)	-	-
[Mn_2(TPAL-DAN)Cl_4]	Brown	200–202	75	663.94	50.48 (51.66)	3.33 (40.1)	8.41 (9.17)	16.49 (17.79)	7.1
[Co_2(TPAL-DAN)Cl_4]	Blue	250-252	85	671.93	49.88 (48.76)	3.29 (3.60)	8.31 (8.28)	17.48 (16.39)	6.7
[Ni_2(TPAL-DAN)Cl_4]	Brown	228–230	95	673.70	49.92 (53.95)	3.29 (3.66)	8.32 (8.78)	17.42 (18.27)	5.0
[Cu_2(TPAL-DAN)Cl_4]	Gray	240–242	87	683.40	49.21 (48.59)	3.24 (3.24)	8.20 (7.97)	18.60 (18.79)	14.3
[Zn_2(TPAL-DAN)Cl_4]	Brown	260–262	76	687.07	48.95 (49.76)	3.24 (3.23)	8.15 (8.15)	19.03 (20.73)	6.5
[Cd_2(TPAL-DAN)Cl_4]	Brown	296–298	89	781.13	43.05 (42.82)	2.84 (3.91)	7.17 (7.17)	28.78 (27.60)	20.6

FTIR Spectrum

The FTIR spectra of the ligand and its metal complexes, which is shown in Table 2 and Fig. S1, unveils distinct vibrational features that elucidate their structural and electronic changes. The free ligand exhibits a characteristic band at 1637 cm^{-1}, assigned to the azomethine group (–C=N–), confirming its formation. In coordination with metal ions, this band undergoes a lower frequency shift in a range of 1627–1631 cm^{-1}, suggestive of a reduction in electron density brought on by the interaction of the metal center with the azomethine nitrogen, confirming its coordinating function [22-23]. Additionally, a broad band at 3297–3337 cm^{-1}, attributed to amino (NH_2) stretching vibrations**,** experiences shift upon complexation, reflecting the participation of the NH_2 group in coordination with the central atom, while the NH_2 band in the ligand at 3346 cm^{-1} [18]. Bands in Table 2 further support the incorporation of nitrogen donor atoms into the coordinating sphere. The bands at (433–475 cm^{-1}) correspond to metal-nitrogen (M–N) stretching [24].

^{1}H- and ^{13}C-NMR Spectra of Ligand

The synthesized ligand's proton ^{1}H-NMR spectrum showed discrete chemical shifts that supported the presence of different functional groups in the spectrum, such as the protons of NH_2 group bonded to the naphthalene group, which exhibited a singlet signal (2H) at 5.65 ppm [24]. The singlet signal at 8.21 ppm corresponds to the proton (1H) of –HC=N group [25]. The chemical shift in the 6.95–7.92 ppm range of the multiplet signals (7H) corresponds to aromatic proton resonances, as shown in Fig. S2(a). The integrals for the protons in the spectrum match the structural formula of the prepared ligand, as shown in Fig. S2(b). Utilizing DMSO-d_6 as the solvent, the ^{13}C-NMR spectrum was obtained, with a strong signal at 141.83 ppm determined to be the carbon atom of the –HC=N group. Additionally, within the chemical shift range of 134.74–106.26 ppm, distinctive signals were observed for aromatic carbon atoms, providing significant structural data about the synthesized ligand. The number of carbon atom signals in the spectrum matches the number of carbon atoms in the chemical formula of the prepared ligand [26-27]. The ^{1}H- and ^{13}C-NMR spectral data of the ligand are summarized in Table 3.

MS Analysis

MS of the ligand was performed to provide strong support for the validity of the predicted molecular structure [28]. The MS showed a characteristic signal at m/z = 414.5 for the molecular ion that matches the molecular weight of the prepared ligand, as shown in Fig. S3. Additionally, it revealed the fragmentation pathways through the presence of characteristic ion peaks, confirming the synthesis process's accuracy and the ligand's structural integrity.

UV-vis Spectrum and Magnetic Studies

At 28250 cm^{-1}, a charge transfer absorption band is visible in the Mn(II) complex (d^5). Five unpaired electrons in a high-spin arrangement are supported by a magnetic moment of 5.60 B.M [29]. Synthesized Co(II) complex (d^7) displays an absorption band at 13860 cm^{-1}, corresponding to $^4A_2(F)\rightarrow{}^4T_1(P)$ transitions at a tetrahedral field, accompanied by a magnetic moment of 4.20 B.M.,

Table 2. FTIR spectral data of the ligand and its complexes

Compounds	νNH_2	νHC=N	νM–N
$C_{28}H_{22}N_4$ (TPAL-DAN)	3346	1637	--
$[Mn_2(TPAL\text{-}DAN)Cl_4]$	3337	1630	441
$[Co_2(TPAL\text{-}DAN)Cl_4]$	3311	1631	475
$[Ni_2(TPAL\text{-}DAN)Cl_4]$	3297	1627	446
$[Cu_2(TPAL\text{-}DAN)Cl_4]$	3330	1630	440
$[Zn_2(TPAL\text{-}DAN)Cl_4]$	3343	1629	433
$[Cd_2(TPAL\text{-}DAN)Cl_4]$	3330	1630	440

Table 3. ^{1}H- and ^{13}C-NMR spectral data of the ligand

^{1}H-NMR	^{13}C-NMR
8.59 (*s*, 1H), 8.21–8.10 (*m*, 1H), 7.97–7.88 (*m*, 2H), 7.58–7.47 (*m*, 1H), 7.32–7.23 (*m*, 1H), 6.82–6.76 (*m*, 3H), 5.65 (*s*, 2H).	141.83, 134.74, 133.79, 129.73, 129.44, 128.34, 128.14, 127.38, 122.70, 116.83, 113.46, 109.21, 106.26.

indicative of pronounced paramagnetism due to three unpaired electrons [30]. The Ni(II) complex (d^8) exhibits a weak absorption band at 14710 cm^{-1}, attributable to $^3T_1(F)\rightarrow{}^3T_1(P)$ transition, with a magnetic moment of 4.30 B.M., reflecting moderate paramagnetism from two unpaired electrons [31]. With a magnetic moment of 1.90 B.M., which is consistent with one unpaired electron, the Cu(II) complex (d^9), which has a tetrahedral shape, exhibits an absorption band corresponding to the $^2Eg\rightarrow{}^2T^2$ g transition. The absence of unpaired electrons is further supported by the tetrahedral geometries of the Zn(II) and Cd(II) complexes, which show no discernible magnetic moment [32]. The unique coordination environments of the synthesized complexes are supported by this evidence. Table 4 provides a detailed description of the electronic spectra data and magnetic characteristics.

Powder XRD Analysis

The elucidation of powder XRD patterns constitutes a pivotal methodology for probing the intricate crystalline attributes of materials [33]. This analytical method is crucial for determining fundamental structural factors, such as particle symmetry, lattice constants, and other intrinsic characteristics shown in Table 5. The comprehensive analysis discerned that hexagonal system, a noteworthy finding given its variety among structurally related Schiff base metal complexes. No secondary crystalline

Table 4. Electronic spectral data on metal complexes, including ligand, and magnetic moments

Compounds	μ_{eff} (B.M)	Absorption (cm^{-1})	Assignment	Suggested structure
$C_{28}H_{22}N_4$ (TPAL-DAN)	-	45789, 41002,	$n\rightarrow\pi^*$, $\pi\rightarrow\pi^*$	-
$[Mn_2(TPAL\text{-}DAN)Cl_4]$	5.60	47870, 41800, 28250	$n\rightarrow\pi^*$, $\pi\rightarrow\pi^*$, C.T	Tetrahedral
$[Co_2(TPAL\text{-}DAN)Cl_4]$	4.20	46442, 32011, 30916, 13860	$n\rightarrow\pi^*$, $\pi\rightarrow\pi^*$, C.T, $^4A_2(F)\rightarrow{}^4T_1(P)$	Tetrahedral
$[Ni_2(TPAL\text{-}DAN)Cl_4]$	4.30	44671, 39611, 29115, 14710	$n\rightarrow\pi^*$, $\pi\rightarrow\pi^*$, C.T, $^3T_1(F)\rightarrow{}^3T_1(P)$	Tetrahedral
$[Cu_2(TPAL\text{-}DAN)Cl_4]$	1.90	46741, 43219, 29917, 12009	$n\rightarrow\pi^*$, $\pi\rightarrow\pi^*$, C.T, $^2Eg(F)\rightarrow{}^2T_2g$	Tetrahedral
$[Zn_2(TPAL\text{-}DAN)Cl_4]$	Dia	47619, 32894, 29411	$n\rightarrow\pi^*$, $\pi\rightarrow\pi^*$, C.T	Tetrahedral
$[Cd_2(TPAL\text{-}DAN)Cl_4]$	Dia	42378, 31645, 29910	$n\rightarrow\pi^*$, $\pi\rightarrow\pi^*$, C.T	Tetrahedral

Table 5. Some crystallographic data from powder XRD of the ligand and some of its prepared complexes

Crystallographic parameters	Mn(II)-complex	Co(II)-complex	Ni(II)-complex	Cu(II)-complex
Crystal system	Hexagonal	Hexagonal	Hexagonal	Hexagonal
Space group	P3221	P3221	P3221	P3221
Space group number	154	154	154	154
Unit cell dimensions	a = 4.9134 α = 90° b = 4.9134 β = 90° c = 4.9134 γ = 120°	a = 4.9130 α = 90° b = 4.9134 β = 90° c = 4.9134 γ = 120°	a = 4.9134 α = 90° b = 4.9134 β = 90° c = 4.9134 γ = 120°	a = 4.9134 α = 90° b = 4.9134 β = 90° c = 4.9134 γ = 120°
Radiation	Cu α rotating anode	Cu α rotating anode	Cu α rotating anode	Cu α rotating anode
Calculated density (g/cm^3)	2.65	2.65	2.65	2.65
Volume of cell (10^6 pm^3)	113.01	113.01	113.01	113.01
Z	3.00	3.00	3.00	3.00
Theta range (°)	13.6961–52.7938	13.2930–77.3930	9.9600–26.2500	16.3060–72.9930
Index ranges	$1 \le h \le 4$ $0 \le k \le 2$ $1 \le L \le 4$	$0 \le h \le 3$ $0 \le k \le 2$ $1 \le L \le 4$	$0 \le h \le 2$ $0 \le k \le 1$ $0 \le L \le 3$	$0 \le h \le 3$ $0 \le k \le 1$ $0 \le L \le 4$

phases were detected, indicating a high degree of phase purity. Although Rietveld refinement was not performed, the sharp diffraction peaks and consistent intensity patterns support the reliability of the structural assignment and suggest a well-ordered crystalline arrangement [34]. The Debye-Scherrer equation, which is expressed as follows, was used to estimate the crystallite dimensions. The size of the crystallite, the shape factor, the incident X-ray wavelength, the full width at half maximum (FWHM) of the diffraction peak as seen in Fig. S4, and the Bragg diffraction angle are all represented in this formulation [35]. Based on the data collected, the resulting calculations showed that the particles produced are in the crystal scale range.

Antioxidant Activity

To evaluate the antioxidant potential of the newly synthesized compounds, their ability to scavenge free radicals was assessed using the *in vitro* (DPPH) assay. Ascorbic acid served as the reference standard for comparison [36-37]. Table 6 illustrates the antioxidant efficacy of the tested compounds, revealing a spectrum of radical scavenging capacities. While some complexes demonstrated superior activity, surpassing the standard, others exhibited moderate to lower efficacy. The synthesized compounds influence their radical neutralization efficiency, thereby dictating their relative performance against DPPH radicals. Structural features, including metal type, geometry, and electronic properties, may significantly influence enzyme activity. Redox-active metals(II) capable of changing oxidation states facilitate essential electron transfer processes for catalytic activity. The coordination geometry around metal ions, whether tetrahedral or octahedral, determines ligand arrangement, which is crucial for substrate binding and orientation, enhancing H-atom or electron donation. The electronic properties of metal centers, shaped by ligands and the environment, dictate reducing or oxidizing abilities, aiding bond changes during catalytic reactions. Understanding these relationships is vital for elucidating mechanisms and has broader implications for drug design and the development of biomimetic catalysts, underscoring the link between structure and function in bio catalysis [38].

Molecular Docking Analysis

The most important inhibitors used to inhibit the 4jlu enzyme are nivolumab [39], adalimumab, and pembrolizumab [40], while a common inhibitor of the 1oxr enzyme is aspirin [41]. The tautomeric forms of ligands at physiological pH (~7.4) affect charge distribution, hydrogen bonding potential, and binding affinity. Negatively charged ligands favor salt bridges and hydrogen bonds with positively charged amino acids like lysine and arginine. Protonated amines enhance interactions with negatively charged residues, while deprotonated forms can facilitate specific hydrogen bonds. These influences affect binding poses and interactions. Generating and docking all relevant tautomeric forms are essential for identifying optimal binding modes, reflecting the ligand's dynamic nature and improving ligand-receptor interaction modeling [42-43].

Molecular docking demonstrated that the synthesized Schiff base ligand and its complexes bonded with different amino acids, forming the target proteins via HC=N, NH_2, and aromatic groups, particularly naphthalene, as well as the interactions induced by the chlorine groups of the central atom of the metal ion. Most interactions of amino acids with aromatic groups

Table 6. Evaluation of ligand and its complexes with DPPH compared to vitamin C

Compounds	200 µg/mL	400 µg/mL	600 µg/mL
(TPAL-DAN)	81	69	67
$[Mn_2(TPAL\text{-}DAN)Cl_4]$	99	92	87
$[Co_2(TPAL\text{-}DAN)Cl_4]$	79	81	81
$[Ni_2(TPAL\text{-}DAN)Cl_4]$	90	88	71
$[Cu_2(TPAL\text{-}DAN)Cl_4]$	88	85	84
Ascorbic acid (vitamin C)	84	86	92

were hydrophobic, in addition to the strong interactions (hydrogen bonds) that many amino acids formed with chloride groups and primary amines when forming the ligand-enzyme complex, which induces inhibition of the target enzyme. Table 7 shows docking with anti-inflammatories and breast cancer receptors' docking scores in a more stable configuration with different medications. Fig. 2 illustrates the various ways that the metal complexes and the protein can bind. Some of these involve hydrogen bonds with the amino acids, while others occur between chlorine atoms and the amino acids. In various types of aromatic systems, pi-pi interactions, hydrophobic bonds, and van der Waals interactions occur. More interactions result in a more stable compound with the protein [44-45]. According to Table 7, the Mn(II) complex had the lowest score value (−9.9667 kcal/mol), suggesting that it is more stable with protein 1oxr. On the other hand, the Zn(II) complex had a lower score value (−8.1601 kcal/mol), indicating that it was more stable with protein 4jlu, as shown in Table 7.

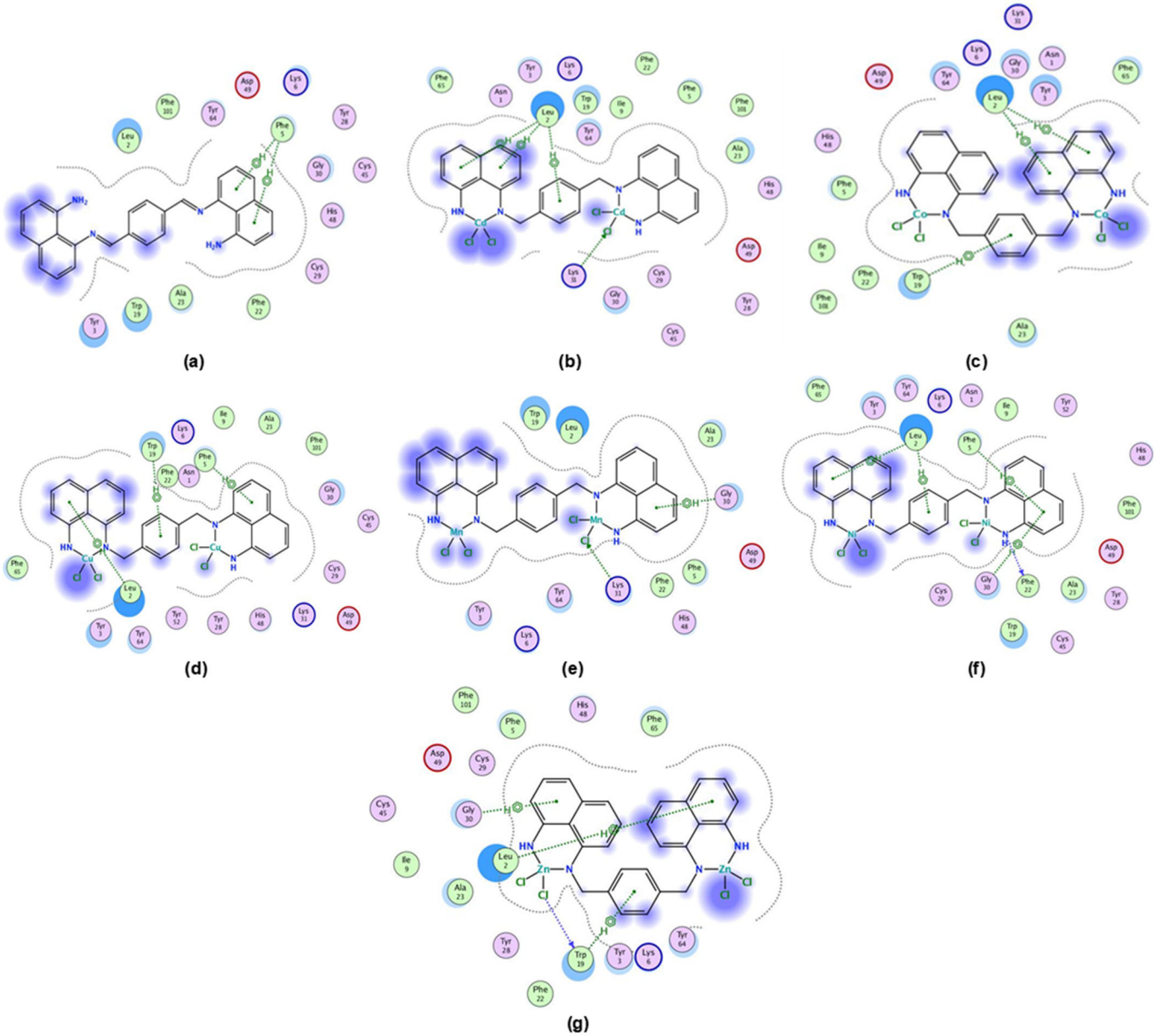

Fig 2. The diagram illustrating the docking of the (a) ligand and (b-g) complexes with the 1oxr protein

Table 7. Scores for docking of the 1oxr and 4jlu proteins of the ligand and its complexes

Compound	1oxr	4jlu
(TPAL-DAN)	−6.8850	−6.1437
$[Mn_2(TPAL\text{-}DAN)Cl_4]$	−9.9667	−6.8741
$[Co_2(TPAL\text{-}DAN)Cl_4]$	−7.6990	−6.7078
$[Ni_2(TPAL\text{-}DAN)Cl_4]$	−7.6107	−6.8119
$[Cu_2(TPAL\text{-}DAN)Cl_4]$	−8.1146	−6.3891
$[Zn_2(TPAL\text{-}DAN)Cl_4]$	−7.6709	−8.1601
$[Cd_2(TPAL\text{-}DAN)Cl_4]$	−7.4047	−7.4110

■ CONCLUSION

The synthesized Schiff base ligand derived from naphthalene 1,8-diamine and terephthalaldehyde exhibited extended conjugation, and six metal complexes were prepared in a 2:1 (M:L) molar ratio, favoring the formation of stable di-nuclear metal complexes with tetrahedral geometry. Physicochemical characterization confirmed the proposed structures. The study of docking against breast cancer and inflammation-related proteins is a highlight of this research, linking experimental chemistry to potential therapeutic applications. Strong binding energies correlate well with antioxidant activity, suggesting a dual function of antioxidant and inhibition of target enzymes. An *in vitro* study comparing the antioxidant results of the prepared Schiff base ligand and its complexes showed that the Mn(II) and Cu(II) complexes had higher free radical scavenging power than the prepared ligand. These results indicate a structure-activity relationship, where the complexes' metal center, coordination geometry, and electronic properties play a crucial role in enhancing radical scavenging through mechanisms such as hydrogen atom or electron donation.

■ ACKNOWLEDGMENTS

The author extends heartfelt appreciation to the Department of Chemistry, College of Sciences, University of Mosul, for their indispensable assistance throughout this research.

■ CONFLICT OF INTEREST

The authors state that there is no conflict of interest.

■ AUTHOR CONTRIBUTIONS

Khansaa Shakir Al-Nama led the development of the conceptual framework, supervised the overall research process, and conducted the interpretation and scientific discussion of the results. Chanar Ahmed Hussein was responsible for designing and executing the experiments, including the synthesis and characterization of the compounds. Ammar Abdulsattar Ibrahim performed the computational studies, specifically the molecular docking simulations, and analyzed the corresponding results. All authors have read and agreed to the final version of this manuscript.

■ REFERENCES

[1] Robson, R., 1970, Complexes of binucleating ligands I. Two novel binuclear cupric complexes, *Inorg. Nucl. Chem. Lett.*, 6 (2), 125–128.

[2] Hoskins, B.F., Robson, R., and Schaap, H., 1972, Complexes of bi nucleating ligands. IV. Some Cu(II) and Ni(II) complexes of 3-formyl-5-methyl-salicylaldehyde di-thiosemicarbazone, *Inorg. Nucl. Chem. Lett.*, 8 (1), 21–25.

[3] Zheng, X., Cheng, W., Ji, C., Zhang, J., and Yin, M., 2020, Detection of metal ions in biological systems: A review, *Rev. Anal. Chem.*, 39 (1), 231–246.

[4] Abdulhameed, Z., and Alabdali, A.J., 2024, Synthesis, characterization and antimicrobial evolution of new bi-α-amino nitrile compounds, *Al-Nahrain J. Sci.*, 26 (4), 21–27.

[5] Rutherford, J.C., and Bird, A.J., 2004, Metal-responsive transcription factors that regulate iron, zinc, and copper homeostasis in eukaryotic cells, *Eukaryotic Cell*, 3 (1), 1–13.

[6] Gennari, M., and Duboc, C., 2020, Bio-inspired, multifunctional metal–thiolate motif: From electron transfer to sulfur reactivity and small-molecule activation, *Acc. Chem. Res.*, 53 (11), 2753–2761.

[7] Muslah, S.I.M., Alabdali, A.J., and Shaalan, N.D., 2020, Synthesis of binuclear bomplexes of Cu(II), Ni(II) and Cr(III) metal ions derived from di-imine compound as bi terminal binding site ligand, *Al-Nahrain J. Sci.*, 23 (4), 19–28.

[8] Hahn, P., Ullmann, S., Klose, J., Peng, Y., Powell, A.K., and Kersting, B., 2020, Dinuclear Tb and Dy complexes supported by hybrid Schiff-base/calixarene ligands: Synthesis, structures and

magnetic properties, *Dalton Trans.*, 49 (31), 10901–10908.

[9] Manhee, T.Q., and Alabdali, A.J., 2024, Synthesis, characterization and anticancer activity of Ni(II), Cu(II), Pd(II) and Au(III) complexes derived from novel Mannich base, *Vietnam J. Chem.*, 62 (2), 201–210.

[10] Tsoupras, A., Pafli, S., Stylianoudakis, C., Ladomenou, K., Demopoulos, C.A., and Philippopoulos, A., 2024, Anti-inflammatory and antithrombotic potential of metal-based complexes and porphyrins, *Compounds*, 4 (2), 376–400.

[11] Alrubaye, A., 2022, Synthesis, characterization and anti-cancer activity of gold(III) and nickel(II) metal ion complexes derived from tetrazole-triazole compound, *Al-Nahrain J. Sci.*, 25 (2), 8–13.

[12] Muslu, H., Kalaycıoğlu, Z., Erdoğan, T., Gölcü, A., and Bedia Erim, F., 2021, Synthesis, characterization, anti-inflammatory evaluation, molecular docking and density functional theory studies of metal-based drug candidate molecules of tenoxicam, *Results Chem.*, 3, 100111.

[13] Ahmed, Y.M., Mahmoud, W.H., Omar, M.M., and Mohamed, G.G., 2021, Synthesis, characterization and biological activity of transition metals Schiff base complexes derived from 4,6-diacetylresorcinol and 1,8-naphthalenediamine, *J. Inorg. Organomet. Polym. Mater.*, 31 (6), 2339–2359.

[14] Mahmoud, W.H., Refaat, A.M., and Mohamed, G.G., 2018, Zinc complexes of novel Schiff bases derived from 1,8-diaminonaphthalene: Synthesis, characterization and biological activity evaluation, *Int. J. Mod. Eng. Res.*, 8 (11), 53–61.

[15] Kadhim, A.J., and Shaalan, N., 2024, Synthesis, characterization, biological, and antioxidant activity of new metal ion complexes with Schiff base derived from 2-hydroxybenzohydrazide, *Indones. J. Chem.*, 24 (6), 1851–1860.

[16] Baliyan, S., Mukherjee, R., Priyadarshini, A., Vibhuti, A., Gupta, A., Pandey, R.P., and Chang, C.M., 2022, Determination of antioxidants by DPPH radical scavenging activity and quantitative phytochemical analysis of *Ficus religiosa*, *Molecules*, 27 (4), 1326.

[17] Startseva, Y.D., Hodyna, D.M., Semenyuta, I.V., Tarasyuk, O.P., Rogalsky, S.P., and Metelytsia, L.O., 2023, Undecylenic acid and *N*,*N*-dibutylundecenamide as effective antibacterials against antibiotic-resistant strains, *Ukr. Biochem. J.*, 95 (4), 55–63.

[18] Sulliman, E.A., Ibrahim, M.A., Ibrahim, A., and Jasim, R.F., 2024, Molecular docking study on tamoxifen and toremifene's effects on the breast cancer receptors, *Turk. Comput. Theor. Chem.*, 8 (4), 62–69.

[19] Al-Burgus, A.F., Thanoon-Ali, O., and Younis Al-Abbasy, O., 2024, Design, synthesis and molecular docking of new spiro heterocyclic coumarin as antibacterial agents, *Rev. Roum. Chim.*, 69 (7-8), 399–404.

[20] Al-Burgus, A.F., Ali, O.T., and Al-Abbasy, O.Y., 2024, New spiro-heterocyclic coumarin derivatives as antibacterial agents: Design, synthesis and molecular docking, *Chim. Techno Acta*, 11 (3), 202411308.

[21] Bansod, A.D., Mahale, R.G., and Aswar, A.S., 2007, Synthesis, characterization, electrical and biological studies on some bivalent metal complexes, *Russ. J. Inorg. Chem.*, 52 (6), 879–883.

[22] Usharani, M., Akila, E., and Rajavel, R., 2013, Coordination of binucleating Schiff base with Cu(II), Co(II), Ni(II) and Mn(II) ions; Designing, structural aspects and pharmacological properties, *Int. J. Med. Pharm. Sci.*, 3 (3), 9–22.

[23] Turan, N., Seymen, H., Gündüz, B., Buldurun, K., and Çolak, N., 2024, Synthesis, characterization of Schiff base and its metal complexes and investigation of their electronic and photonic properties, *Opt. Mater.*, 148, 114802.

[24] Khalil, E.A.M., Mahmoud, W.H., El Dessouky, M.M.I., and Mohamed, G.G., 2021, Synthesis, spectral, thermal and biological studies of some transition and inner transition Schiff base metal complexes, *Egypt. J. Chem.*, 64 (7), 3555–3571.

[25] Tomar, D., Chaurasia, M., Tyagi, P., Agrawal, S., Kumar, P., Sharma, D., Chhikara, A., and Chandra, S., 2021, Synthesis, characterization, antimicrobial, MTT assay, DFT study of Co(II), Ni(II), Cu(II) and

Zn(II) complexes with some new Schiff base ligands, *Egypt. J. Chem.*, 64 (9), 4995–5008.

[26] Ferretti, F., Rota, L., and Ragaini, F., 2021, Unexpected coordination behavior of ruthenium to a polymeric α-diimine containing the poly[*bis*(arylimino)acenaphthene] fragment, *Inorg. Chim. Acta*, 518, 120257.

[27] Al-Hialy, Q.H., and Al-Nama, K.S., 2021, Synthesis, antibacterial activity and DFT calculation of Co(II) and Ni(II) Schiff bases complexes derived from acenaphthenequinon and phenylenediamine, *Egypt. J. Chem.*, 64 (11), 6429–6438.

[28] Shaalan, N., Khalaf, W.M., and Mahdi, S., 2022, Preparation and characterization of new tetra-dentate N_2O_2 Schiff base with some of metal ions complexes, *Indones. J. Chem.*, 22 (1), 62–71.

[29] Paswan, S., Anjum, A., Singh, A.P., and Dubey, R.K., 2019, Synthesis and spectroscopic characterization of lanthanide complexes derived from 9,10-phenanthrenequinone and Schiff base ligands containing N, O donor atoms, *Indian J. Chem., Sect. A*, 58A, 446–453.

[30] Kowalkowska-Zedler, D., Nedelko, N., Kazimierczuk, K., Aleshkevych, P., Łyszczek, R., Ślawska-Waniewska, A., and Pladzyk, A., 2020, Novel tetrahedral cobalt(II) silanethiolates: Structures and magnetism, *RSC Adv.*, 10 (49), 29100–29108.

[31] AL-Nama, K.S., Saeed, I.A., and Mohammed, A.F., 2025, Synthesis, characterization, DFT, molecular docking, and *in vitro* screening of metal chelates incorporating Schiff base, *Bull. Chem. Soc. Ethiop.*, 39 (4), 687–701.

[32] Liu, Y., Ube, H., Endo, K., and Shionoya, M., 2023, Temperature-dependent spontaneous resolution of a tetrahedral chiral-at-nickel(II) complex under supramolecular control, *ACS Org. Inorg. Au*, 3 (6), 371–376.

[33] Aly, S.A., Hassan, S.S., El-Boraey, H.A., Eldourghamy, A., Abdalla, E.M., Alminderej, F.M., and Elganzory, H.H., 2024, Synthesis, biological activity, and the effect of ionization radiation on the spectral, XRD, and TGA analysis of Cu(I), Cu(II), Zn(II), and Cd(II) complexes, *Arabian J. Sci. Eng.*, 49 (1), 361–379.

[34] Thomas, P.S., Philip, S., and Mohanan, K., 2017, Synthesis and spectroscopic characterization of some transition metal complexes of Schiff base 3-(2-hydroxyphenylimino)methyl-4,5-dimethyl-1-phenylpyrazol-3-in-2-one, *Orient. J. Chem.*, 33 (6), 2787–2795.

[35] Inac, H., Ashfaq, M., Dege, N., Feizi-Dehnayebi, M., Munawar, K.S., Yağcı, N.K., Poyraz Çınar, E., and Tahir, M.N., 2024, Synthesis, spectroscopic characterizations, single crystal XRD, supramolecular assembly inspection via Hirshfeld surface analysis, and DFT study of a hydroxy functionalized Schiff base Cu(II) complex, *J. Mol. Struct.*, 1295, 136751.

[36] Guo, G., Saidi, T.L., Terban, M.W., Valsecchi, M., Billinge, S.J.L., and Lipson, H., 2025, Ab initio structure solutions from nanocrystalline powder diffraction data via diffusion models, *Nat. Mater.*, 2025, s41563-025-02220-y.

[37] Cornea, A.C., Marc, G., Ionuț, I., Moldovan, C., Stana, A., Oniga, S.D., Pîrnău, A., Vlase, L., Oniga, I., and Oniga, O., 2025, Synthesis, characterization, and antioxidant activity evaluation of new *N*-methyl substituted thiazole-derived polyphenolic compounds, *Molecules*, 30 (6), 1345.

[38] Kumar, R., Shikha, D., and Sinha, S.K., 2024, DPPH radical scavenging assay: A tool for evaluating antioxidant activity in 3% cobalt–doped hydroxyapatite for orthopaedic implants, *Ceram. Int.*, 50 (8), 13967–13973.

[39] Abdullah, W., Nik Ab Razak, N.N.A., Dheyab, M.A., Salem, F., Abdul Aziz, A., Alanezi, S.T., Oladzadabbasabadi, N., and Ghasemlou, M., 2025, Melanin-driven green synthesis and surface modification of metal and metal-oxide nanoparticles for biomedical applications, *Adv. Funct. Mater.*, 2 (50), 30–17.

[40] Schmid, P., Cortes, J., Pusztai, L., McArthur, H., Kümmel, S., Bergh, J., Denkert, C., Park, Y.H., Hui, R., Harbeck, N., Takahashi, M., Foukakis, T., Fasching, P.A., Cardoso, F., Untch, M., Jia, L., Karantza, V., Zhao, J., Aktan, G., Dent, R., and O'Shaughnessy, J., 2020, Pembrolizumab for early triple-negative breast cancer, *N. Engl. J. Med.*, 382 (9), 810–821.

[41] Barbee, M.S., Ogunniyi, A., Horvat, T.Z., and Dang, T.O., 2015, Current status and future directions of the immune checkpoint inhibitors ipilimumab, pembrolizumab, and nivolumab in oncology, *Ann. Pharmacother.*, 49 (8), 907–937.

[42] Steiner, M.A., Sciarretta, C., Pasquali, A., and Jenck, F., 2013, The selective orexin receptor 1 antagonist ACT-335827 in a rat model of diet-induced obesity associated with metabolic syndrome, *Front. Pharmacol.*, 4, 165.

[43] Li, F., Eriksen, J., Oses-Prieto, J.A., Gomez, Y.K., Xu, H., Hareendranath, S., Das, P., Finer-Moore, J., Nguyen, P., Bowen, A., Nelson, A., Burlingame, A., Grabe, M., Stroud, R.M., and Edwards, R.H., 2025, Substrate recognition and allosteric regulation of synaptic vesicle glutamate transporter VGLUT2, *Nat. Struct. Mol. Biol.*, 2025, s41594-025-01568-8.

[44] Kukić, P., and Nielsen, J.E., 2010, Electrostatics in proteins and protein–ligand complexes, *Future Med. Chem.*, 2 (4), 647–666.

[45] Vasanthi, V., Gunasekaran, S., Dhanalakshmi, E., Rajesh, P., Kesavan, M., Kumaresan, L., Almutairi, S.M., and Bin Talha, N.T., 2025, Spectroscopic, solvent interactions, topological analysis, docking evaluation with biological studies on 1,3,3-trimethyl-2-oxybicyclo[2.2.2] octane by anti-cancer proteins, *J. Mol. Struct.*, 1321, 139689.